An experimental investigation into the effects of rotation on the isothermal flow resistance in circular tubes rotating about a parallel axis

A. R. Johnson* and W. D. Morris†
*Department of Mechanical and Process Engineering, University of Sheffield, Sheffield, England
†Department of Mechanical Engineering, University of Wales, University College of Swansea, Swansea, Wales

Results are presented of an experimental investigation into the influence of rotation on the flow resistance of a circular sectioned tube rotating about an axis parallel to its central axis of symmetry. This investigation is part of a long-term study into the effect of rotation on pressure loss and heat transfer characteristics in rotating coolant channels. Analytical examination of the governing conservation equations indicate that for isothermal flow rotation will have no effect on the fully developed flow apart from a cross-stream hydrostatic pressure gradient due to additional centripetal acceleration terms in the equations; this has been verified experimentally. In the entrance region the effects of the additional centripetal acceleration terms would be manifest solely as a hydrostatic pressure field; this was also verified experimentally. In the entrance region analytical examination of the governing conservation equations predict Coriolis-induced secondary flows. The existence of Coriolis-induced effects in the entrance region have been experimentally verified, increases in the friction factor being noted that were correlated using the rotational Reynolds number, which is a measure of the relative strength of Coriolis to viscous forces.

Keywords: turbomachines; gas turbines; flow resistance

Introduction

Machine components that rotate while subjected to a relatively high temperature environment must often be internally cooled in order to ensure reliable operation. The rotors of medium-to-high power electrical motors or generators and the rotor blades of aero gas turbines are notable examples. In these circumstances, where coolant is constrained to flow inside rotating channels, it is necessary to determine how the rotation modifies the flow field and the consequential flow resistance and heat transfer so that an adequate design assessment of cooling performance may be made. This problem arises not only in the coolant passages within the component but also in any rotating ducting that transmits the coolant to that component.

The present paper reports experimental data that demonstrate the manner in which rotation alters the pressure drop experienced by an isothermal fluid flowing in a circular-sectioned tube that rotates about an axis parallel to, but displaced from, its symmetry axis. This rotating flow geometry is shown in Figure 1 and is referred to as parallel-mode rotation for convenience throughout the paper. As well as its fundamental interest, the work has relevance to the design of cooling systems for electrical machine rotors and rotor windings.

Address reprint requests to Dr. Johnson at the Dept. of Mechanical and Process Engineering, University of Sheffield, P.O. Box 600, Mappin Street, Sheffield S1 3JD, UK.

Received 24 October 1990; accepted 30 September 1991

© 1992 Butterworth–Heinemann

The expected influence of tube rotation may be explained by reference to the momentum conservation equations, and this is done in the following section. These theoretical observations were used to formulate a series of exploratory experiments (Johnson 1988 and Johnson and Morris 1984), which led to more detailed studies reported here.

Theoretical considerations

In this section, a qualitative assessment of the effect of parallel-mode rotation on the tube flow is presented via an examination of the momentum and vorticity conservation equations. For steady isothermal laminar flow in a tube that rotates uniformly about an arbitrary axis the momentum conservation equation takes the form (Morris 1981a and Johnson 1988)

$$\frac{D\mathbf{v}}{Dt} + 2(\boldsymbol{\omega} \times \mathbf{v}) + \boldsymbol{\omega} \times (\boldsymbol{\omega} \times \mathbf{r}) + \mathbf{a}_o = -\frac{1}{\rho}\nabla p + \nu\nabla^2\mathbf{v} \qquad (1)$$

where $\mathbf{v}$ is the fluid velocity vector measured relative to a reference frame that moves with the tube, $\mathbf{r}$ is the position vector of a general point in the flow relative to this moving frame, $\boldsymbol{\omega}$ is the angular velocity vector of the tube in space, and $\mathbf{a}_o$ is the absolute acceleration of the origin of the frame of reference, i.e., the centerline of the tube. Additionally, in Equation 1, p is the fluid pressure and ρ and ν are the constant fluid density and kinematic viscosity, respectively. The operator D/Dt is the usual total derivative.

The last two terms on the left-hand side of Equation 1, originating from the acceleration of the origin of the noninertial reference frame adopted and the centripetal acceleration component due to rotation, are conservative. They are made manifest solely by a cross-stream hydrostatic pressure gradient (Morris 1981a and Johnson 1988).

The vorticity equation governs the generation of vorticity and its subsequent convection and diffusion through the fluid. With a rotating fluid system an additional source term for the generation of relative vorticity exists and has its origin in the Coriolis component of acceleration, namely $2(\omega \times \mathbf{v})$ in Equation 1 (Morris 1981a and Johnson 1988).

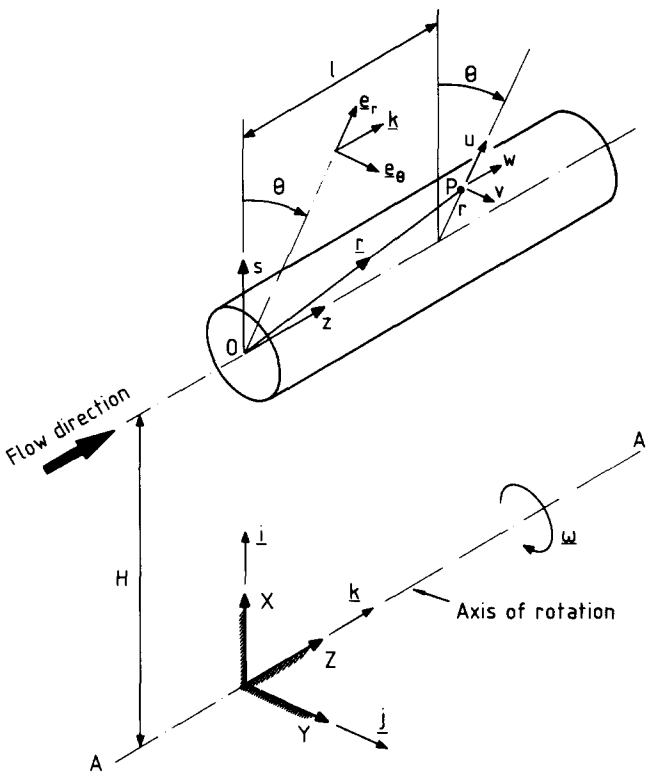

Figure 1 Flow geometry and coordinate systems

Examination of the vorticity equation demonstrates that relative vorticity will only be generated in a tube rotating in the parallel mode if axial gradients of velocity exist. Once the flow has developed, the axial gradients of velocity by definition vanish and so rotation has no effect on the flow field other than a hydrostatic pressure field to support the centripetal-type terms in the original momentum equation. The influence of rotation will thus be confined to the entrance regions of the tube where axial gradients of velocity exist.

Coriolis-driven secondary flows generated in the entrance region will depend on the form of velocity distribution in the immediate entry plane of the tube itself. Additionally, the entry plane velocity distribution depends on the way in which the fluid is delivered to the entry plane. If this is done by means of rotating ducting, then it may be argued that the actual flow in the tube of interest is a function of the delivery system adopted.

A finite difference solution of Equation 1 for laminar and turbulent pipe flow with parallel-mode rotation (Johnson 1988) suggested that the interaction of the Coriolis force and the developing velocity field is not strong. Although the growth and subsequent decay of a swirling flow component was confirmed, it did not have a significant influence on the development of the axial velocity component or the axial pressure drop when compared with the stationary pipe flow behavior. The entry plane velocity profile assumed for the numerical solution of the governing equations involved a uniform axial velocity with no cross-stream secondary flow. In practice, far more complex entry plane velocity distributions are likely due to the fact that the fluid will be presented to the tube via ducting, which itself is subjected to rotation; further numerical modeling may lead to this pressure increase being predicted. For this reason, an experimental investigation (Johnson and Morris 1984) of the pressure loss in the entry region of tubes rotating in the parallel mode was undertaken to systematically examine its sensitivity to rotation, geometric parameters, and entry plane flow conditioning.

Nondimensional parameters that describe the flow system geometry, rotation, and flow field may be easily derived from an examination of the momentum conservation equations (Johnson and Morris 1982 and Johnson 1988). Accordingly, the following parameters have been used for the presentation

Notation

$\mathbf{a}_o$	Acceleration of tube axis
C_f	Friction factor, $\left(\dfrac{\Delta p\, d}{0.5\rho w_m^2 l}\right)$
C_{fL}	Friction factor for fully developed laminar flow through a stationary tube, $\left(\dfrac{64}{\mathrm{Re}}\right)$
C_{fT}	Friction factor for fully developed turbulent flow through a stationary tube, $(0.316\,\mathrm{Re}^{-0.25})$
d	Tube diameter
e	Eccentricity ratio
$\mathbf{e}_r, \mathbf{e}_\theta, \mathbf{k}$	Unit vectors for cylindrical coordinates
H	Tube eccentricity
$\mathbf{i}, \mathbf{j}, \mathbf{k}$	Unit vectors for Cartesian coordinates
l	Distance along tube
J	Rotational Reynolds number, $\left(\dfrac{\Omega d^2}{\nu}\right)$
p	Pressure
Δp	Static pressure drop along tube
$\mathbf{r}$	Position vector of fluid particle relative to cylindrical coordinates
r, θ, z	Cylindrical coordinates, fixed to tube
Re	Reynolds number, $\left(\dfrac{w_m d}{\nu}\right)$
u, v, w	Radial, tangential, and axial fluid velocities relative to tube
$\mathbf{v}$	Fluid velocity vector relative to tube
w_m	Mean axial fluid velocity

Greek symbols

ν	Fluid kinematic viscosity
ρ	Fluid density
ω	Angular velocity vector

of the experimental data, which follows.

$$\frac{l}{d} \quad \text{(length/diameter ratio of the tube)}$$

$$e = \frac{H}{d} \quad \text{(eccentricity parameter)} \qquad (2)$$

$$\mathrm{Re} = \frac{w_m d}{\nu} \quad \text{(pipe flow Reynolds number)}$$

$$\mathrm{J} = \frac{\Omega d^2}{\nu} \quad \text{(rotational Reynolds number)}$$

The rotational Reynolds number may be interpreted as a measure of the relative strength of Coriolis to viscous forces.

Investigative details

Previous exploratory experiments (Johnson and Morris 1982, Johnson and Morris 1984, and Johnson 1988) have confirmed some of the rotational effects suggested by the qualitative examination of the governing conservation equations. In this respect the following general conclusions were drawn from these initial series of experiments.

(1) Parallel-mode rotation did not produce any significant change in the axial pressure loss when the flow was developed. This was true with laminar and turbulent flow.
(2) Rotation was found to give a more gradual transition from laminar to turbulent developed flow in comparison with the well-known dip that occurs in the friction factor/Reynolds number relationship with transitional flow in stationary tubes.
(3) Although not fully confirmed, it was apparent that the pressure loss was not dependent on the eccentricity ratio. This would be the case if the centripetal effect was entirely hydrostatic.
(4) The pressure loss was sensitive to the geometry of the inlet plenum chamber used when rotation was included; for relatively unsmoothed inlets the increases were large. As the inlet flow was progressively conditioned using gauzes and straightening tubes in the inlet plenum, so the effect of rotation was reduced.
(5) It was confirmed that rotation increased the pressure loss when tubes of short aspect ratio were used. This tended to confirm generation of Coriolis-induced swirl in the developing flow regimes, as explained in the previous section.

As a result of these preliminary findings it was decided to undertake a more systematic study of this flow geometry, with the following strategic aims.

(1) To assess the sensitivity of the pressure loss to the rotational Reynolds number parameter. In the preliminary experiments the rotational speed was held constant. This resulted in the rotational Reynolds number parameter increasing at the higher flow rates due to an increase in the density of the air in the test section. Since the rotational Reynolds number would appear to be an important parameter, the detailed experiments were conducted, holding this parameter constant by adjusting the rotational speed accordingly.
(2) To assess the effect of the axial length along the tube on the development of the pressure loss. In the preliminary experiments the five pressure tappings were located at 150-mm intervals along each of the different diameter test sections, resulting in a wide range of length/diameter ratios. In order to assess the axial development of the pressure loss the pressure tappings were located at identical length/diameter ratios from the entrance of the test section for each of the different diameter tubes used in the detailed experiments.
(3) To check that the flow resistance was not affected by the eccentricity parameter.
(4) To correlate the experimental results using the parameters suggested by the theoretical considerations, and given by Equation set 2.

Test facility

The test facility used for this investigation is outlined in Figure 2 and was designed to permit easy attachment of a variety of test section modules to a basic supporting rotor, with minimized disturbance to the drive system and instrumentation. The salient component or subassembly features of the facility are indicated by number on the diagram.

A flanged shaft (14), supported on two bearings (7), permitted assorted test section modules (9) to be attached in the parallel-mode attitude via five rotor arms (20). This overall rotor assembly was driven by means of a controlled motor (17) and a toothed belt pulley system (18). Air could be pumped through the test module from a regulated compressed air supply via rotary seals (6, 11) mounted on the outboard side of each of the main bearings. The air was delivered to the test section through the radial connecting tube (13), with a similar arrangement for exhausting the air on exit from the test section. Dynamic balance of the assembled rotor was achieved using adjustable balancing weights (16) fitted diametrically opposite the test module on the supporting rotor arms. The eccentricity of the test section relative to the axis of rotation could be varied by changing the supporting rotor arms. Two sets of rotor arms were available giving eccentricities of 305 and 457 mm.

As described earlier, the strategic aim of this investigation was to examine the manner in which pressure drop along the tube was affected by tube geometry, inlet delivery geometry, flow rate, and rotation. To this end the various test configurations used were designed into a basic modular structure as typified by Figure 3. In simplistic terms the test section modules consisted of a straight circular-sectioned tube (A) over which the pressure drop measurements were taken. The tubes had an overall length of 646 mm and three different diameters (6.86, 10.23, and 14.17 mm) were used during the

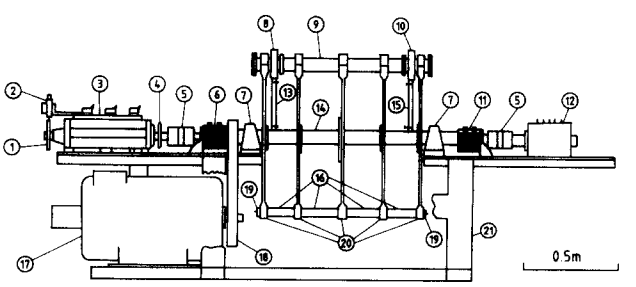

1. Tachometer disc
2. Tachometer pick up
3. Thermocouple slip ring assembly
4. Thermocouple connector disc
5. Flexible coupling
6. Inlet rotary air seal
7. Main bearing
8. Inlet plenum chamber
9. Test section module
10. Exit plenum chamber
11. Exit rotary air seal
12. Pressure transmission unit
13. Inlet radial connecting tube
14. Main rotor shaft
15. Exit radial connecting tube
16. Spacing sleeves (coarse balancing masses)
17. Variable speed motor
18. Toothed pulley belt drive
19. Fine balancing masses
20. Rotor arms
21. Supporting framework

Figure 2 Schematic layout of the experimental apparatus

detailed investigation. This tube was supported on flanged extension pieces (B), which were themselves attached to inlet and exit plenum chambers, (C) and (D), respectively. The extension piece on the inlet side incorporated the geometrically different inlet configurations, which were tested as part of the main strategic investigation (Johnson and Morris 1984). Details of the most smoothed inlet from that investigation, which was used in the detailed experimental investigation reported here, are given in Figure 4. The area reduction in the bell mouth for each diameter test section was kept constant at a value of 6.82. This was achieved by the use of the carefully cast and polished bronze-loaded epoxy inserts shown in Figure 4. For each test section the pressure tappings were located at length/diameter ratios of 10.6, 21.2, 31.8, and 42.3, these being measured from the first pressure tapping that had a short calming length of 1.6 diameters prior to it from the true inlet of the test section at plane *ZZ* in Figure 4. Further, pressure drop measurements over the final pressure tap span gave an indication of the best approach to fully developed flow and had a calming length prior to this span of 33.4 diameters from the test section inlet at plane *ZZ*.

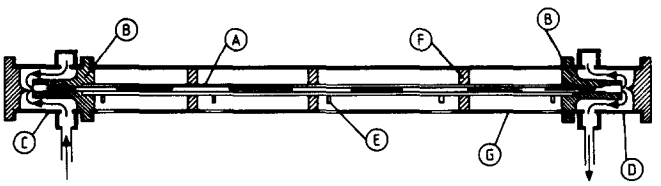

Figure 3 Schematic layout of the test section module

The pressure of the air flowing along the test section could be measured at five axial locations by means of conventional hydrostatic pressure tappings connected to a range of Furness micromanometers (accuracy ± 1 percent fsd) or mercury U tube manometers as appropriate. The novelty of this system of measurement involved the manner in which the pressure signals were taken from the rotating tube to the stationary measuring instruments. The principle of the method used is shown in Figure 5. The pressures at two typical points A and B on the tube were connected to sealed chambers C and D, through which the main rotor shaft passed. Provided an adequate seal is maintained between the rotating shaft and the casing of the sealing chambers, then the pressure drop from A to B on the test section can be measured by connecting the two chambers to a stationary pressure measuring device. This idea was incorporated into a five-channel pressure transmission unit that was attached to one end of the main rotor assembly (see item 12 in Figure 2). Completely leak-proof sealing between the rotor and the chambers was achieved by means of a magnetic oil held in the small radial clearance between the shaft and casing. This magnetic oil was held in place by creating a strong magnetic field in the clearance gap with permanent magnets built into the casing assembly. The pressure transmission system, and the overall flow circuit, could be checked for leaks by isolating and pressurizing the portion under test, any leaks being indicated by a reduction in pressure. It is important to note that this procedure could be conducted with the test facility rotating. Fuller details of this pressure transmission technique may be found elsewhere (Johnson 1988 and Morris 1981b).

The flow rate through the test section was measured using one of four calibrated Fischer 2000 series rotameter flow meters located downstream of the rotor immediately before the air was exhausted to atmosphere. The temperature of the air entering the test section was measured using a copper/constantan thermocouple with the thermoelectric signal taken from

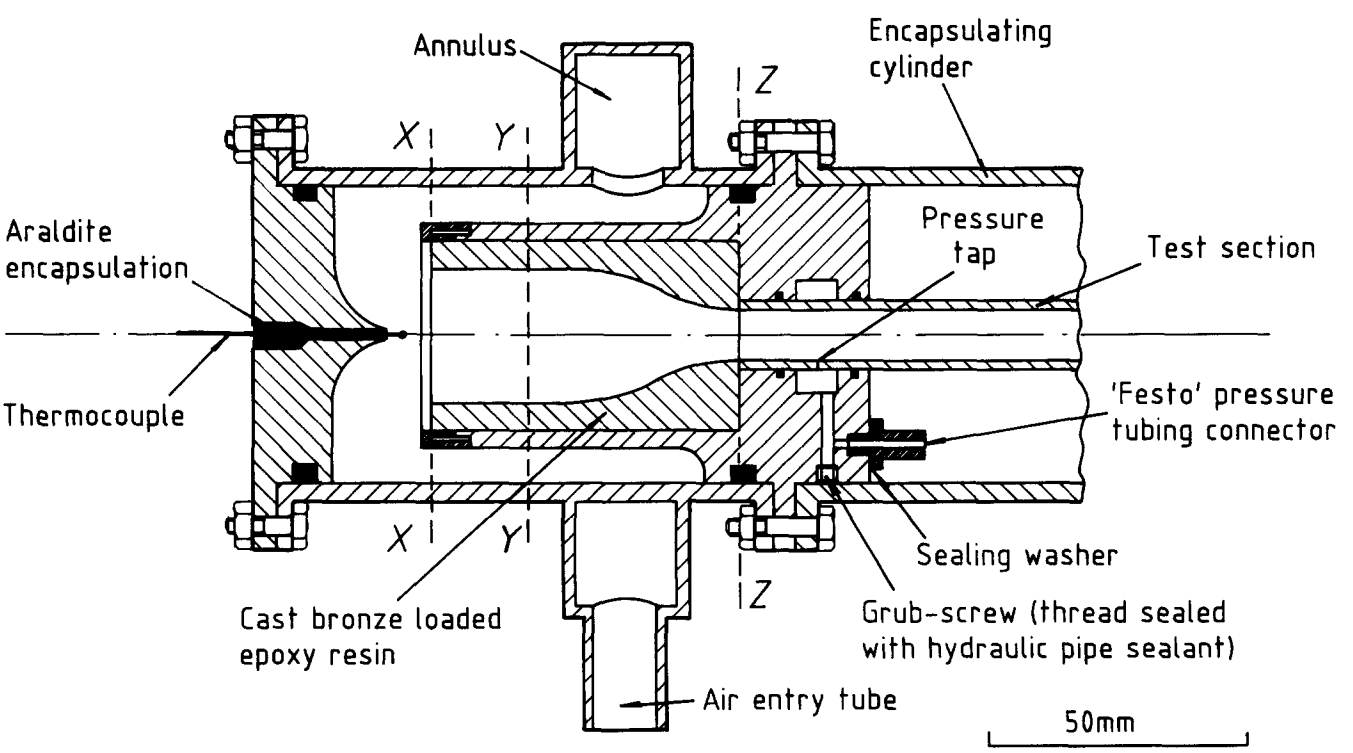

Figure 4 Inlet plenum chamber assembly

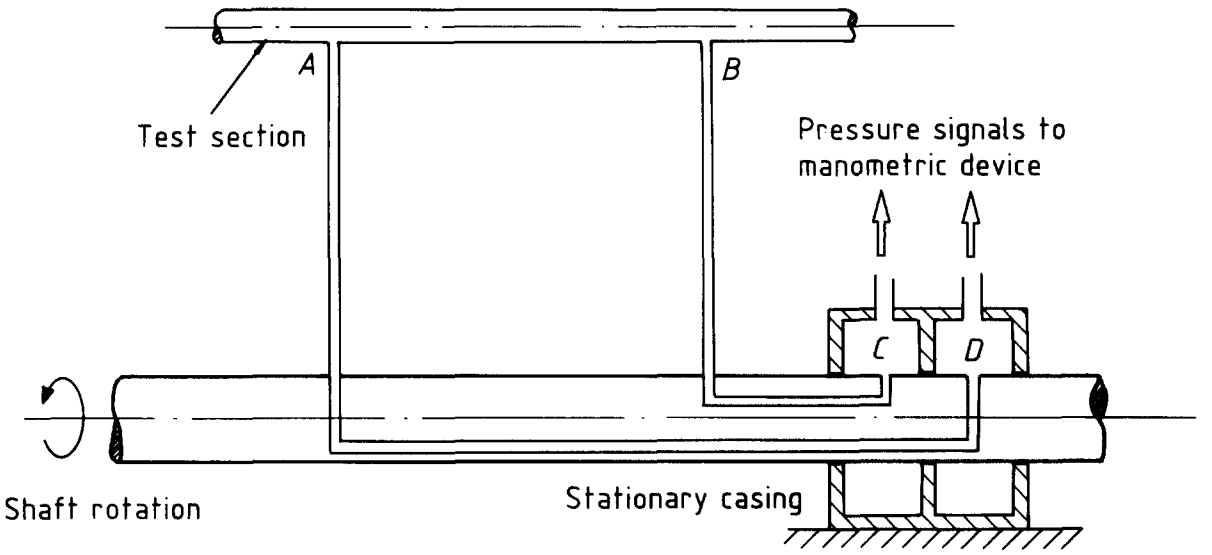

Figure 5 Principle of the pressure measurement system

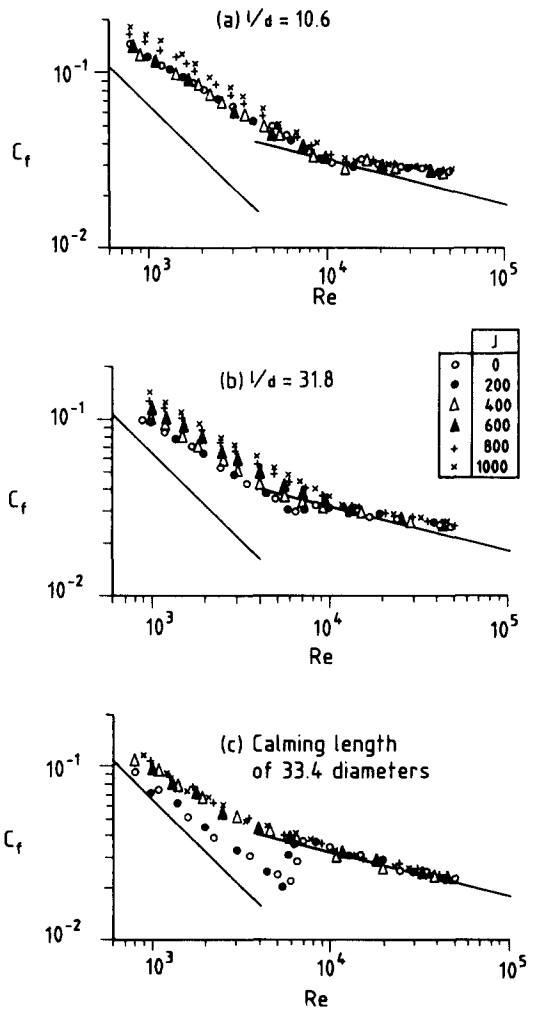

Figure 6 Typical effect of rotation on the friction factor in the entrance region (14.17-mm diameter test section, 457 mm eccentricity)

the rotor via a silver/silver-graphite slip ring shown at 3 in Figure 2. The speed of the rotor was measured using a magnetic encoder and timer counter fitted to the end of the slip ring assembly at 1 and 2 in Figure 2.

All instrumentation signals needed for the investigation were transmitted either manually or automatically to a Solatron System 35 data acquisition system for recording. This facility was also used for the subsequent analysis of the data and the output of results.

Results and discussion

Results are presented for the friction factor C_f based on the static pressure drop Δp along the tube, namely

$$C_f = \frac{\Delta p\, d}{0.5\rho w_m^2 l} \tag{3}$$

In order to assist in the interpretation of the results, the standard correlations for fully developed flow through a stationary tube are shown in the figures. These are

$$\text{Laminar flow } C_{fL} = \frac{64}{\text{Re}} \tag{4}$$

$$\text{Turbulent flow } C_{fT} = 0.316\,\text{Re}^{-0.25} \tag{5}$$

Examination of the instrumentation accuracy and the experimental errors (Johnson 1988) indicated that the typical error in the friction factor was ± 15 percent for notionally laminar flow ($\text{Re} < 2000$) and ± 10 percent for notionally turbulent flow ($\text{Re} > 5000$). The experimental values obtained were, however, repeatable typically within ± 5 percent. Adequate functioning of the apparatus and the data logging and processing techniques were verified by first obtaining results with the rotor stationary.

The typical effect of rotation on the friction factor at various rotational Reynolds numbers is shown in Figure 6 for the largest 14.17-mm diameter test section with the larger 457-mm radius rotor arms. The friction factors are presented for length/diameter ratios of 10.6 and 31.8 and for the best approach to fully developed flow, which had a prior calming length of 33.4

diameters. At the lowest rotational Reynolds number of 200, rotation has a negligible effect on the friction factor; however, there appears to be a slight indication that rotation is causing transition to turbulent flow at a slightly lower Reynolds number value for the best approximation to fully developed flow shown in Figure 6c. It should be emphasised that although for a rotational Reynolds number of 200 the effects on the friction factor are negligible, this does not mean that there are no significant rotational effects. This has been illustrated in the numerical predictions (Johnson 1988), which showed that while rotation had a negligible effect on the friction factor, it nevertheless produced a significant axisymmetric swirling flow, which increases in the entrance region before decaying away when the flow becomes fully developed. This swirling flow may lead to increased pressure losses in subsequent fittings in the flow circuit.

In the entrance region shown in Figure 6a rotation has a negligible effect on the turbulent friction factor, i.e., for Reynolds numbers in excess of 15,000, which confirms the numerical predictions that rotation would have little effect on the turbulent friction factor (Johnson 1988). For Reynolds numbers less than 15,000 and rotational Reynolds numbers less than 600 there is also negligible effect on the friction factor. However, for the higher rotational Reynolds numbers of 800 and 1000 there are clear increases, particularly for laminar flow, say for Reynolds numbers less than 5000. The numerical predictions (Johnson 1988) indicated that rotation had a negligible effect on the laminar friction factor, even though a significant axisymmetric swirling flow was predicted. However, an ideal nonswirling uniform inlet velocity profile was assumed, which would clearly not have been the case in the experimental investigation, even with a smoothed inlet. This was shown in the inlet configuration investigation (Johnson and Morris 1984) in which large increases in friction factor were observed with a relatively unsmoothed inlet. These increases were reduced by flow-straightening devices in the bell-mouth, the most smoothed inlet being used in the present investigation. It is, therefore, likely that particularly at the higher rotational speeds, significant rotational effects from the upstream flow still remain after the flow-straightening devices in the inlet. These residual rotational effects are the most likely cause of the increases in friction factor in the entrance region shown in Figure 6a. It should also be emphasized that Coriolis-generated rotational effects will modify the flow between the end of the flow-straightening honeycomb at plane YY and the inlet of the test section at plane ZZ shown in Figure 4. In this region there will be significant axial gradients of velocity, which have been shown to be precisely the condition for Coriolis-generated secondary flows to develop. Thus, even if the velocity profile at plane YY was uniform and nonswirling, which is not likely, at the inlet to the test section at plane ZZ some Coriolis-generated secondary flow would have developed. Further, any residual rotational and entry effects at plane YY would have been further modified.

The numerical predictions (Johnson 1988) indicated that for laminar flow the swirling velocity reached a peak after 13 diameters for a Reynolds number of 1000, increasing to 26 diameters for a Reynolds number of 2000. For turbulent flow the peak was reached after 8.5 diameters for a Reynolds number of 10,000, increasing to 12.7 diameters for a Reynolds number of 50,000. It is probable then that, particularly for laminar flow, rotational effects will still be increasing during and after the first pressure tap span of 10.6 diameters, for which the results are presented in Figure 6a. It may be anticipated, therefore, that the friction factor for a longer portion of the tube would show more discernable rotational effects. This is precisely what is seen in Figure 6b, which illustrates the effects of rotation for a length/diameter ratio of 31.8 and where clear increases in friction factor are now evident for rotational Reynolds numbers in excess of 400 for Reynolds numbers below 12,000. Although in the turbulent region for Reynolds numbers greater than 12,000, rotation has a negligible effect on the friction factor.

The effect on the best approach to fully developed flow is shown in Figure 6c. It has been argued that the residual entrance effects become less important further away from the inlet and that the numerical and theoretical predictions that rotation has no effect on fully developed flow are more likely to be observed. This is clearly seen in Figure 6c where for turbulent flow, i.e., for Reynolds numbers in excess of 6000, rotation has a negligible effect on the friction factor. Further, for Reynolds numbers less than 6000 the data all fall into a tight band for rotational Reynolds numbers greater than 400. However, this is significantly above the results for the stationary tube and for a rotational Reynolds number of 200, which are virtually coincident. It should, however, be emphasized that the flow is unlikely to be fully developed at this length/diameter ratio for laminar flow. Results for test sections with calming lengths greater than 75 (Johnson and Morris 1982) indicated that for these more fully developed cases that rotation had negligible effect for Reynolds numbers less than about 1500. However, the more gradual transition from laminar-like to turbulent-like flow shown in Figure 6c was also apparent.

An aim of the detailed investigation was to examine the axial development of the pressure loss along the tube by examining results for different diameter test sections, but that had pressure tappings at the same length/diameter ratios from the entrance. Typical results for all the constant length/diameter test sections, using both the 305- and 457-mm rotor arms, are shown in Figures 7 and 8 for rotational Reynolds numbers of 0 and 600, respectively. As expected, the results for the stationary test section show that for a particular length/diameter ratio the results for the different diameter test sections are essentially identical. This is also the case for the rotational case shown in Figure 8 for a rotational Reynolds number of 600. This clearly illustrates that the pressure drop development is defined by the length/diameter ratio along the test section from the entrance.

It was argued in the theoretical considerations section that the centripetal terms in the governing momentum equations do not create secondary flows but are made manifest only by a hydrostatic pressure distribution across the tube, and therefore have no effect on the friction factor. These centripetal terms are the only ones to include the eccentricity of the tube, and so this parameter is likely to be an unimportant one. The results of the exploratory experiments (Johnson and Morris 1982 and Johnson and Morris 1984) suggested that the eccentricity parameter was relatively unimportant in its effects on the pressure loss and so tentatively confirmed the theoretical predictions. However, several parameters in these experiments varied by ± 6 percent from the nominal values quoted and so details of a more rigorous experimental investigation using physically different eccentricities available from 305- and 457-mm radius rotor arms are now presented.

The results shown in Figures 7 and 8 cover a wide range of test section eccentricity ratios and clearly show that the effect of the eccentricity is negligible over the complete range of experimental Reynolds numbers, thus confirming the theoretical predictions that the eccentricity has no effect on the friction factor.

An attempt to correlate the increase in friction factor due to rotation would give an indication of the relative importance of the various controlling parameters derived earlier and given by Equation set 2. In order to achieve this the largest 14.17-mm diameter test section was used because this gave the widest range of rotational Reynolds number values of 0–1000. Further, it has clearly been shown in Figures 7 and 8 that the results for the other test sections at a given rotational Reynolds number

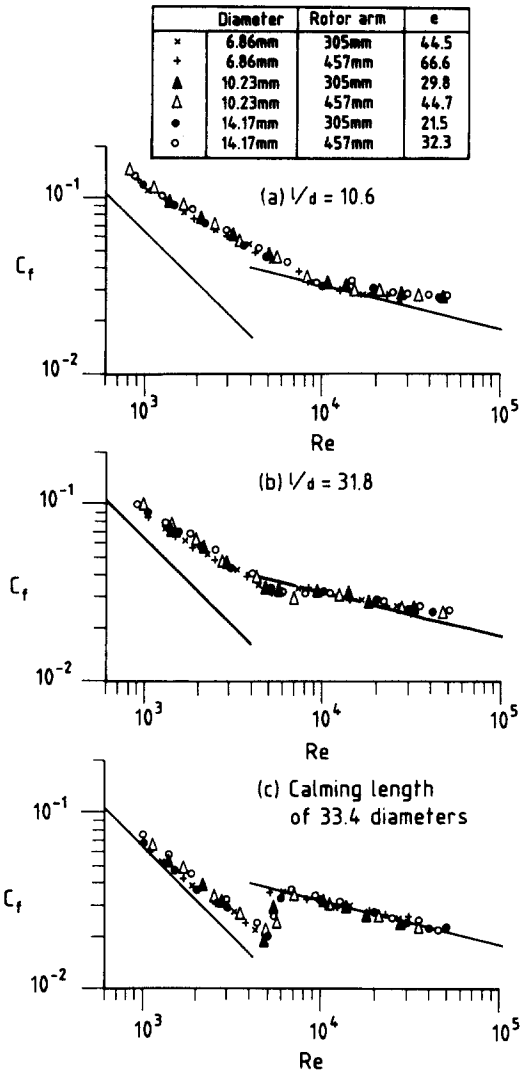

Figure 7 Comparison of the friction factors at a rotational Reynolds number of 0 (i.e., stationary) using the two different diameter rotor arms (6.86-, 10.23-, and 14.17-mm diameter test sections)

and length/diameter ratio are effectively the same. Additionally, it has been confirmed that the eccentricity ratio is an unimportant parameter. The other rotational parameter in Equation set 2 is the rotational Reynolds number. This rotational parameter was, therefore, used in an attempt to correlate the experimental results.

The results for length/diameter ratios of 10.6 and 31.8 are presented in Figure 9, using the ratio of the rotational Reynolds and the Reynolds number as correlating factors. The results for all rotational Reynolds numbers fall within fairly tight bands. However, for the shortest length/diameter ratio of 10.6 shown in Figure 9a, there are some small systematic variations within the band. These differences may be due to residual upstream effects that have not been fully smoothed by the inlet flow-straightening devices and that are likely to vary with rotational speed. However, after the inlet these residual effects will tend to decay and will also be further modified by Coriolis effects. Thus, the differences with rotational speed may be expected to diminish further along the test section. This is confirmed for the larger length/diameter ratio of 31.8 shown in Figure 9b where the systematic variations have virtually disappeared.

The data shown in Figure 9 show a fairly distinct change in slope, and this may be considered as the change from laminar-like to turbulent-like flow. The data may then be correlated to within approximately ± 10 percent using an equation of the following form and with the constants and validity range given in Table 1:

$$C_f = aJ^b \, \mathrm{Re}^c \tag{6}$$

Due to the mathematical structure of Equation 6, it does not apply at zero rotational speed. Indeed, examination of Figure 6 reveals that the results for a rotational Reynolds number of 200 are effectively coincident with those at zero rotational speed. It is, therefore, suggested that for rotational Reynolds numbers less than 200, the stationary correlations shown in Figure 10 are used. These are given by an equation of the following form and the constants and validity range are given in Table 2:

$$C_f = x \, \mathrm{Re}^y \tag{7}$$

The accuracy of Equations 7.1–7.4 are approximately ± 5 percent. It is interesting to note that the discrepancy for a rotational Reynolds number of 200 between using Equations 6.1–6.4 and the corresponding one of Equations 7.1–7.4 is typically under 5 percent.

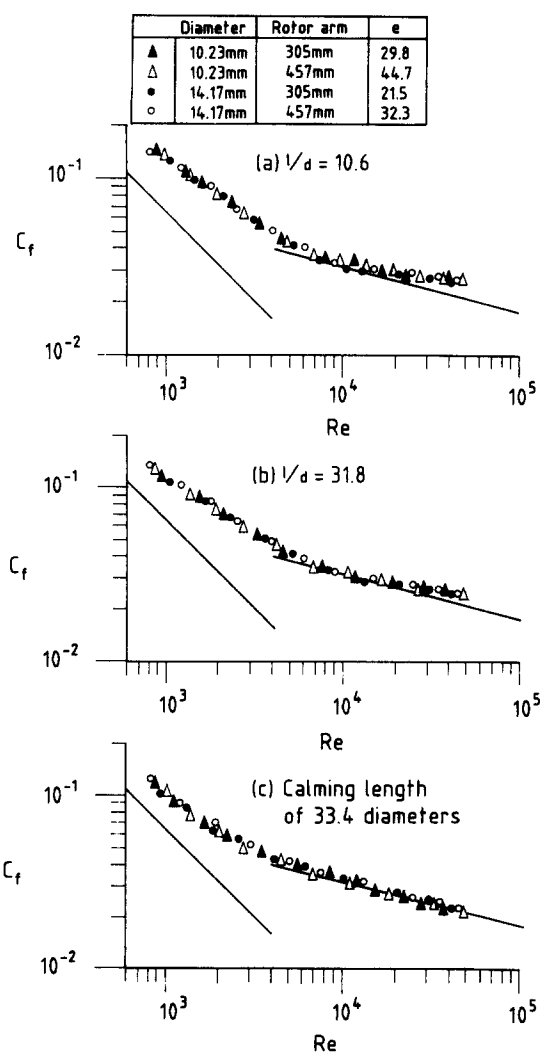

Figure 8 Comparison of the friction factors at a rotational Reynolds number of 600 using the two different diameter rotor arms (6.86-, 10.23-, and 14.17-mm diameter test sections)

Using Equations 6.1–6.4 the increase in friction factor for a rotational Reynolds number of 1000 compared with 200 are typically

length/diameter ratio of 10.6
laminar-like flow +30 percent
turbulent-like flow +4 percent

length/diameter ratio of 31.8
laminar-like flow +40 percent
turbulent-like flow +10 percent

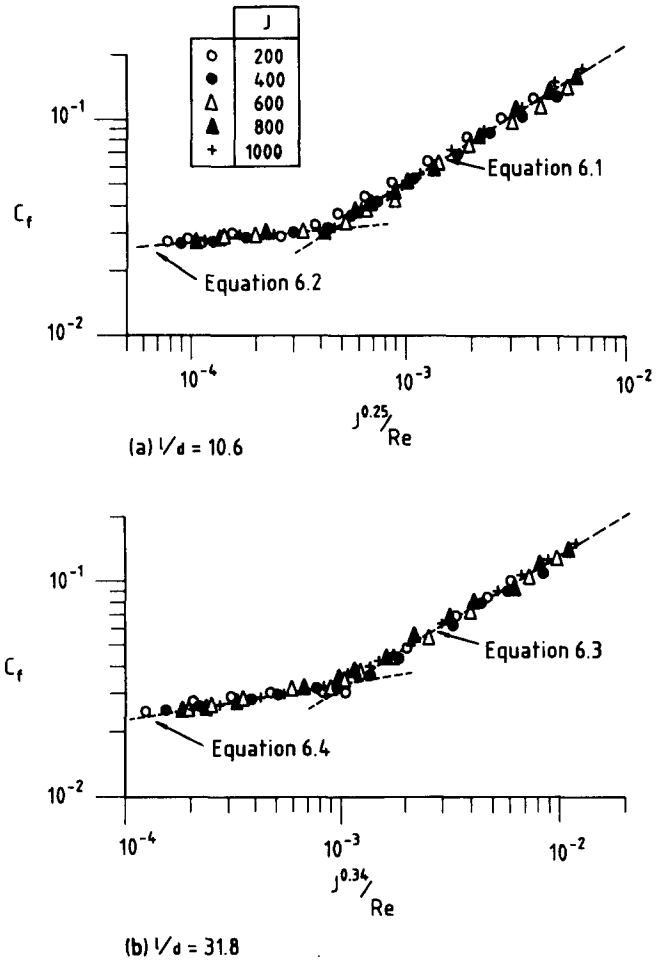

Figure 9 Correlations for the effect of rotation on the friction factor (14.17-mm diameter test section)

These results confirm that for turbulent flow, rotation has little effect on the friction factor, and thus use of the appropriate stationary correlations 7.2 and 7.4 would be adequate. However, it should be stressed that these correlating equations only apply to the smoothed inlet configuration. With a relatively unsmoothed inlet used in earlier investigations (Johnson and Morris 1982 and Johnson and Morris 1984) very marked increases in friction factor were evident.

Concluding remarks

Examination of the governing momentum conservation equation indicates that three additional terms are required to

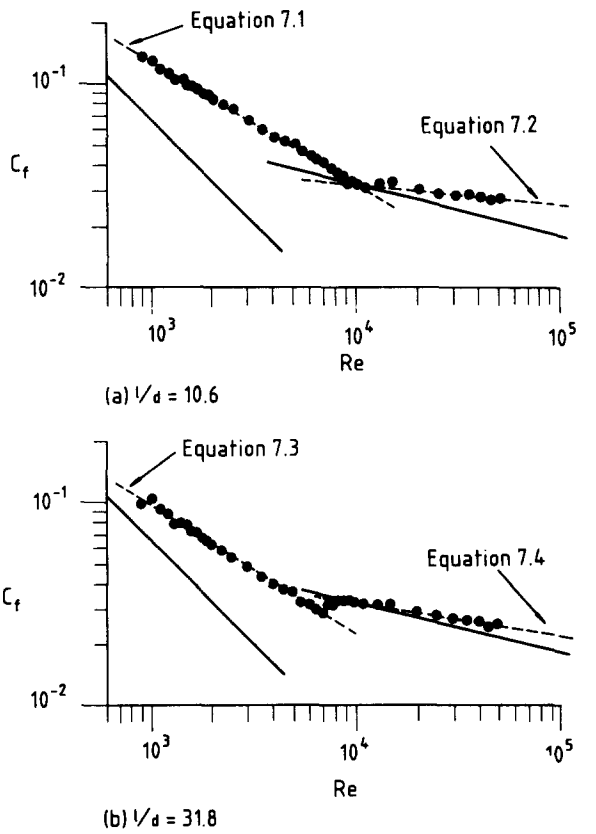

Figure 10 Correlations for the stationary friction factor for the 14.17-mm diameter test section

Table 1 Constants and range of validities for use in Equation 6, for rotational Reynolds numbers of 200–1000

Equation No.	$\frac{l}{d}$	Flow type	*a*	*b*	*c*	Validity range
6.1	10.6	Laminar-like	3.98	0.16	−0.63	$4.57 \times 10^{-4} < \frac{J^{0.25}}{Re} < 6.0 \times 10^{-3}$
6.2	10.6	Turbulent-like	0.064	0.023	−0.093	$7.5 \times 10^{-5} < \frac{J^{0.25}}{Re} < 4.57 \times 10^{-4}$
6.3	31.8	Laminar-like	2.30	0.21	−0.62	$1.12 \times 10^{-3} < \frac{J^{0.34}}{Re} < 1.2 \times 10^{-2}$
6.4	31.8	Turbulent-like	0.108	0.058	−0.17	$1.2 \times 10^{-4} < \frac{J^{0.34}}{Re} < 1.12 \times 10^{-3}$

Table 2 Constants and range of validities for use in Equation 7 for a rotational Reynolds number of 0 (i.e., stationary)

Equation No.	$\frac{l}{d}$	Flow type	x	y	Validity range
7.1	10.6	Laminar	7.91	−0.60	$900 < Re < 9880$
7.2	10.6	Turbulent	0.076	−0.095	$9880 < Re < 51{,}000$
7.3	31.8	Laminar	7.37	−0.63	$900 < Re < 7000$
7.4	31.8	Turbulent	0.138	−0.16	$8000 < Re < 51{,}000$

describe isothermal flow through a parallel-mode tube. These are, firstly, the acceleration of the centerline of the tube; secondly, a centripetal acceleration term; and thirdly, a Coriolis acceleration term. The first two of these additional terms are made manifest solely as a cross-tube hydrostatic pressure gradient similar to that due to the earth's gravitational field. This has been verified experimentally where it was shown that the eccentricity parameter that describes these two terms had no discernable effect on the friction loss.

The Coriolis term acts as a source term for the generation of vorticity relative to the tube, provided there are axial gradients of velocity, i.e., when the flow is developing in the entrance region of the tube. The presence of these Coriolis-induced effects was demonstrated experimentally where increases in flow resistance were noted in the entrance region. Further, these increases were successfully correlated using the rotational Reynolds number, which is a measure of the relative strengths of Coriolis to viscous forces. When the flow becomes fully developed, rotation does not generate any secondary flow and the only difference to flow through a stationary tube is the cross-tube hydrostatic pressure distribution due to the first two additional terms. This has been verified experimentally in this investigation although some details have been reported elsewhere (Johnson and Morris 1982 and Johnson and Morris 1984).

It also has been demonstrated that the axial development of the friction factor along the tube is defined by the length/diameter ratio from the tube entrance.

The experimental increases in flow resistance due to rotation in the entrance region were typically about 30–40 percent in the laminar flow region, but under 10 percent in the turbulent region. However, it should be emphasized that these results were for the smoothed inlet used in this investigation, for relatively unsmoothed inlets large increases in friction factor have been observed and have been reported earlier (Johnson and Morris 1982 and Johnson and Morris 1984). In particular designers of rotating cooling circuits should be aware that rotation may in some circumstances result in significant increases in flow resistance in comparison with those predicted using stationary correlations. Thus, the use of stationary correlations, or stationary experimental simulations, for the design of rotating cooling circuits may lead to an overestimation of the flow through a particular rotating channel and hence lead to an underestimation of the cooling provided. This error may lead to a premature failure of the machine.

Acknowledgments

The authors would like to express their appreciation to the Central Electricity Research Laboratories of the Central Electricity Generating Board and the Science and Engineering Research Council for financial support for conducting this program of work. The experimental data were obtained while the authors were members of staff in the Department of Engineering Design and Manufacture, University of Hull.

References

Johnson, A. R. 1988. Flow resistance in circular tubes rotating about a parallel axis. Ph.D. thesis, University of Hull, UK

Johnson, A. R. and Morris, W. D. 1982. Pressure loss measurements in circular ducts which rotate about a parallel axis. *Proc. XIV ICHMT Symposium on Heat Transfer in Rotating Machinery*, Dubrovnik, Yugoslavia

Johnson, A. R. and Morris, W. D. 1984. Experimental investigation of the effect of entry conditions and rotation on flow resistance in circular tubes rotating about a parallel axis. *Int. J. Heat Fluid Flow*, **5**, 121

Morris, W. D. 1981a. *Heat Transfer and Fluid Flow in Rotating Coolant Channels*. Res. Studies Press, John Wiley & Sons, New York

Morris, W. D. 1981b. A pressure transmission system for flow resistance measurements in a rotating tube. *J. Phys. Sci. Instrum.*, **14**, 208